

## ***Supporting Information***

# **Band-Bowing Effects in Lead-Free Double $\text{Cs}_2\text{AgBi}_x\text{Sb}_{1-x}\text{Cl}_6$ Perovskites and Their Anion-Exchanged Derivatives**

**Oleksandr Stroyuk<sup>1\*</sup>, Oleksandra Raievskaya<sup>1</sup>, Anastasia Barabash<sup>2</sup>,  
Riley W. Hooper<sup>3</sup>, Vladimir K. Michaelis<sup>3</sup>,  
Jens Hauch<sup>1,2</sup>, Christoph J. Brabec<sup>1,2</sup>**

<sup>1</sup>*Forschungszentrum Jülich GmbH, Helmholtz-Institut Erlangen Nürnberg für Erneuerbare Energien  
(HI ERN), 91058 Erlangen, Germany*

<sup>2</sup>*Friedrich-Alexander-Universität Erlangen-Nürnberg, Materials for Electronics and Energy Technology (i-MEET),  
Martensstrasse 7, 91058 Erlangen, Germany*

<sup>3</sup>*Department of Chemistry, University of Alberta, 11227 Saskatchewan Drive, Edmonton, Alberta, Canada T6G 2G2*

### **Author for correspondence:**

\*Dr. Oleksandr Stroyuk, Forschungszentrum Jülich GmbH, Helmholtz-Institut Erlangen Nürnberg für Erneuerbare Energien (HI ERN), Immerwahrstr. 2, 91058 Erlangen, Germany; *e-mail:* o.stroyuk@fz-juelich.de, alstroyuk@ukr.net.

## Tables

**Table S1.** Composition of Cs-Ag-Bi-Sb-Cl perovskites from EDX analysis

Nominal Bi fraction $x$	Actual Bi fraction $x_a$	Cl/(Bi+Sb)	Cs/(Bi+Sb)	Ag/(Bi+Sb)
0	0	5.56	1.96	1.00
0.05	0.06	5.55	2.02	1.00
0.10	0.12	5.36	1.93	0.98
0.25	0.26	5.06	1.91	0.92
0.50	0.50	4.92	1.87	0.92
0.75	0.76	5.18	1.86	0.90
0.90	0.91	5.02	2.02	0.91
1.00	1.00	5.42	1.96	0.96

**Table S2.** Composition of the products of Cl-to-Br anionic exchange in CABSC perovskites

Bi/(Bi+Sb)	Cs/(Bi+Sb)	Ag/(Bi+Sb)	Na/(Bi+Sb)	(Br+Cl)/(Bi+Sb)	Br/(Br+Cl)
0	1.51	0.68	0.13	4.70	0.64
0.07	1.53	0.86	0.12	4.45	0.65
0.12	1.47	0.36	0.14	4.60	0.65
0.25	1.68	1.04	0.19	5.55	0.66
0.47	1.89	0.97	0.27	5.90	0.68
0.82	1.96	1.02	0.18	6.00	0.67
0.94	1.97	1.00	0.25	6.05	0.68
1.00	2.01	1.04	0.21	5.80	0.68

**Table S3.** Composition of Cs-Bi-Sb-I perovskites from EDX analysis

Nominal Bi fraction $x$	Actual Bi fraction $x_a$	I/(Bi+Sb)	Cs/(Bi+Sb)
0	0	4.57	1.48
0.05	0.07	4.24	1.47
0.10	0.12	4.27	1.44
0.25	0.29	3.94	1.43
0.50	0.52	4.50	1.52
0.75	0.78	4.61	1.54
0.90	0.88	4.75	1.55
1.00	1.00	4.87	1.59

## Figures

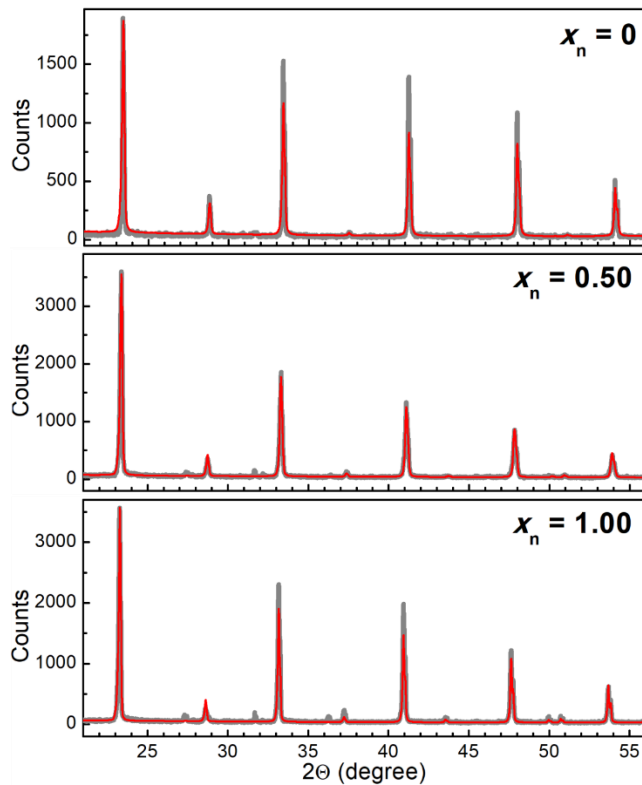


**Figure S1.** XRD patterns of  $\text{Cs}_2\text{AgBi}_x\text{Sb}_{1-x}\text{Cl}_6$  perovskites with a nominal Bi fraction  $x_n$  of 0, 0.50, and 1.00 (gray lines) and Rietveld refinement of the experimental data (red lines).

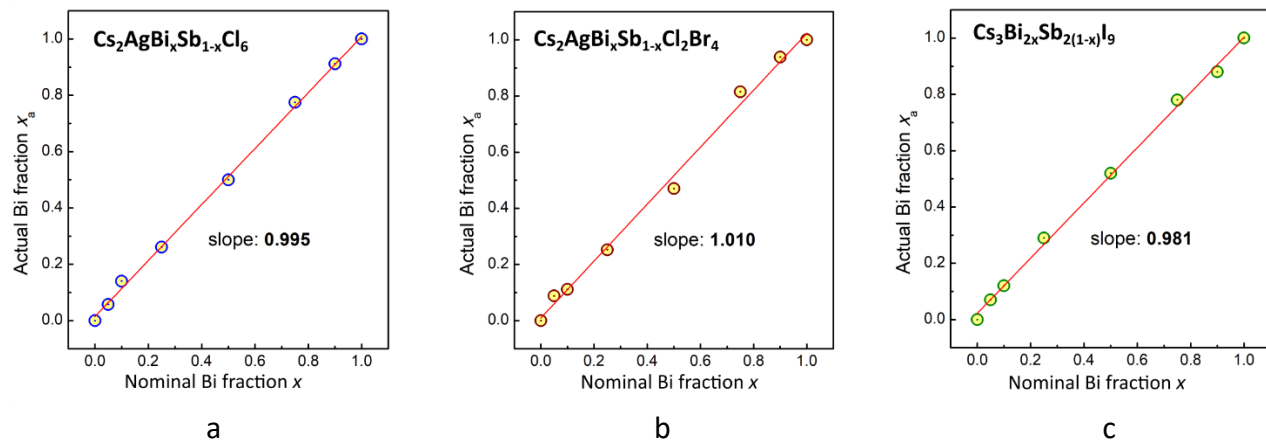


**Figure S2.** Actual Bi fraction  $x_a$  versus nominal Bi fraction  $x$  for original  $\text{Cs}_2\text{AgBi}_x\text{Sb}_{1-x}\text{Cl}_6$  double perovskites (a) and the products of anion exchange with NaBr (b) and NaI (c).

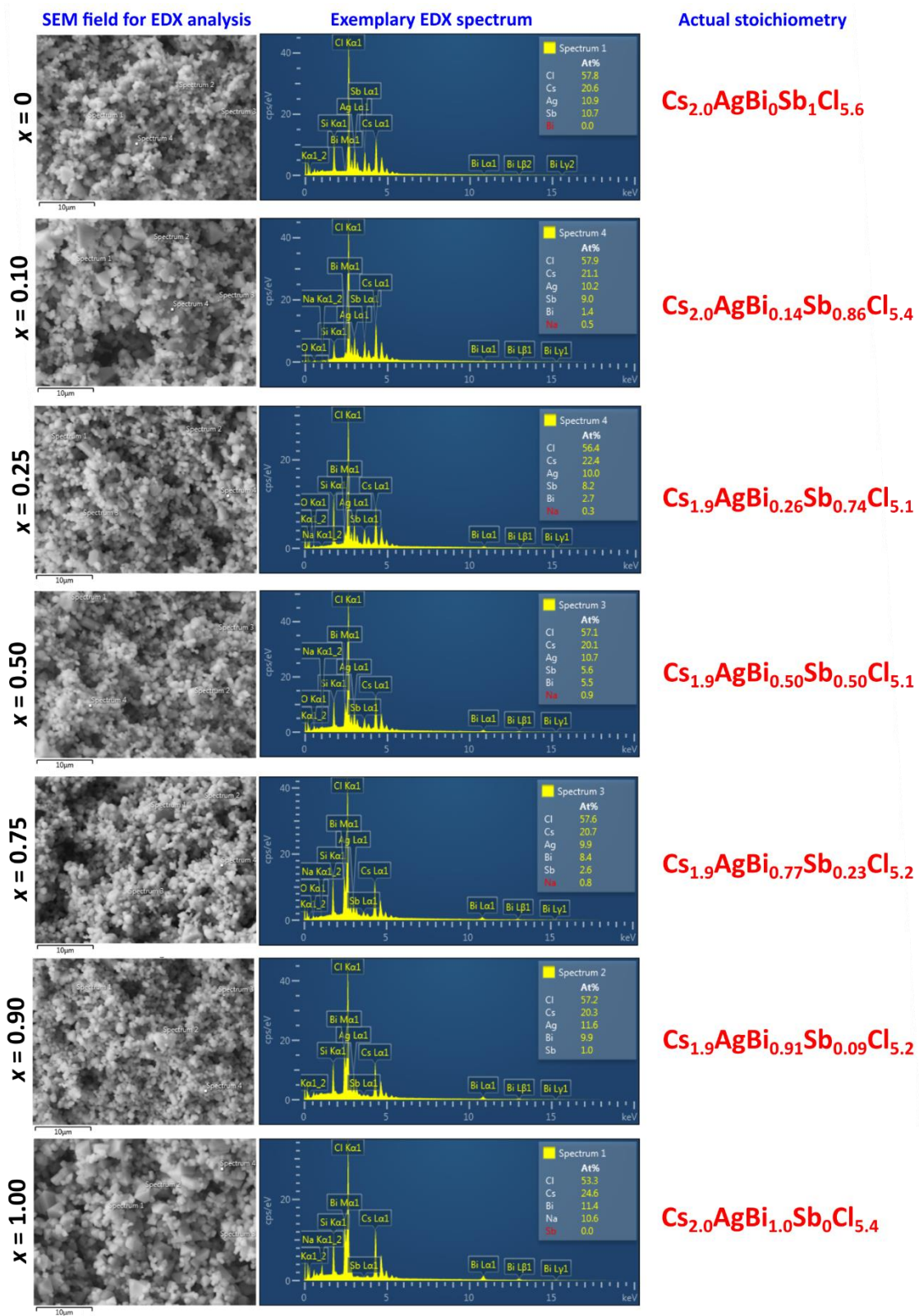


**Figure S3.** SEM of sample areas used for the EDX analysis, exemplary EDX spectra, and actual stoichiometries derived from EDX data for  $\text{Cs}_2\text{AgBi}_x\text{Sb}_{1-x}\text{Cl}$  perovskites.

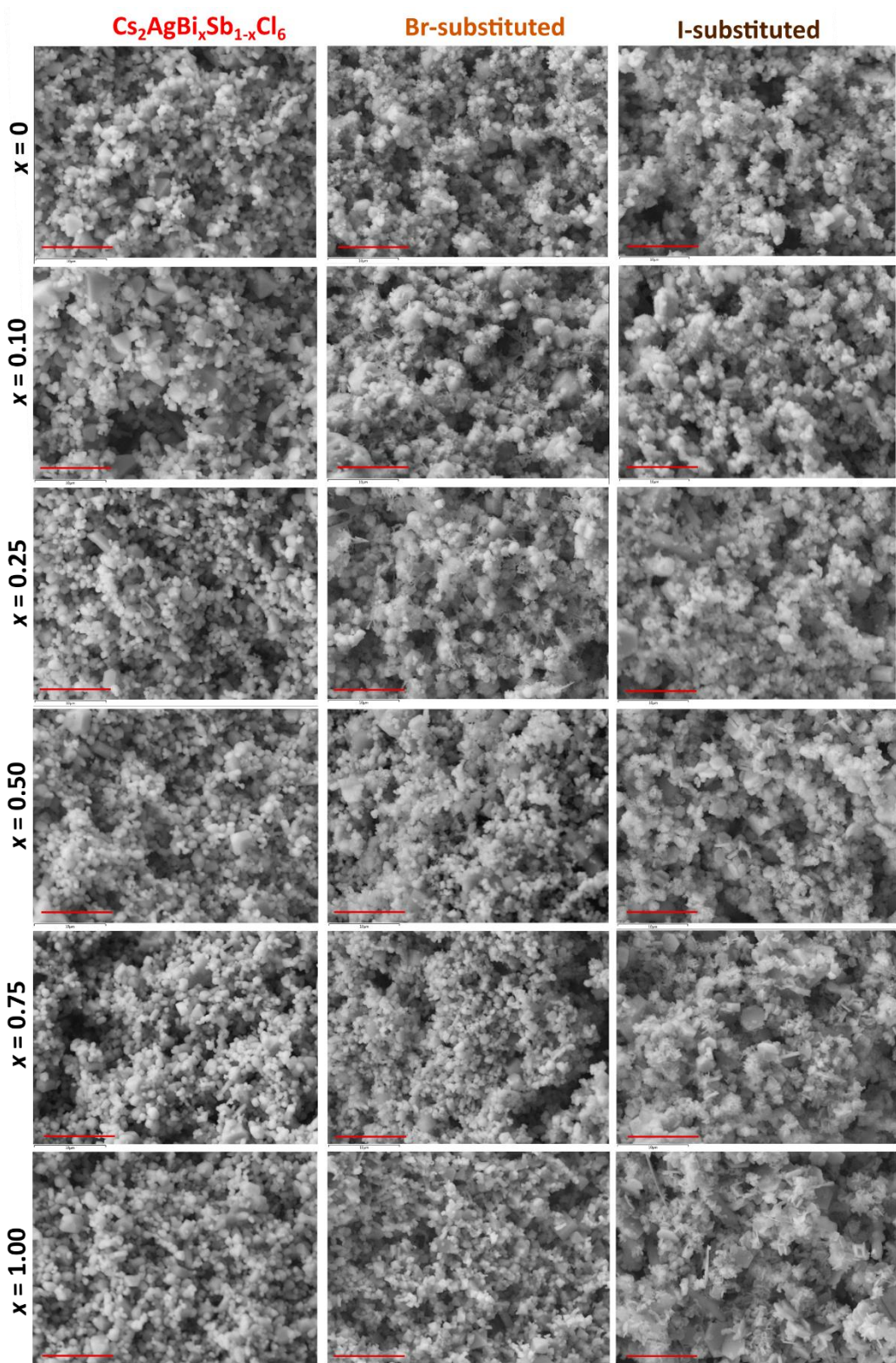


**Figure S4.** SEM images of  $\text{Cs}_2\text{AgBi}_x\text{Sb}_{1-x}\text{Cl}_6$  double perovskites with varied  $x$  and corresponding products of Br-to-Cl and I-to-Cl substitution. The scale bar is 10  $\mu\text{m}$ .

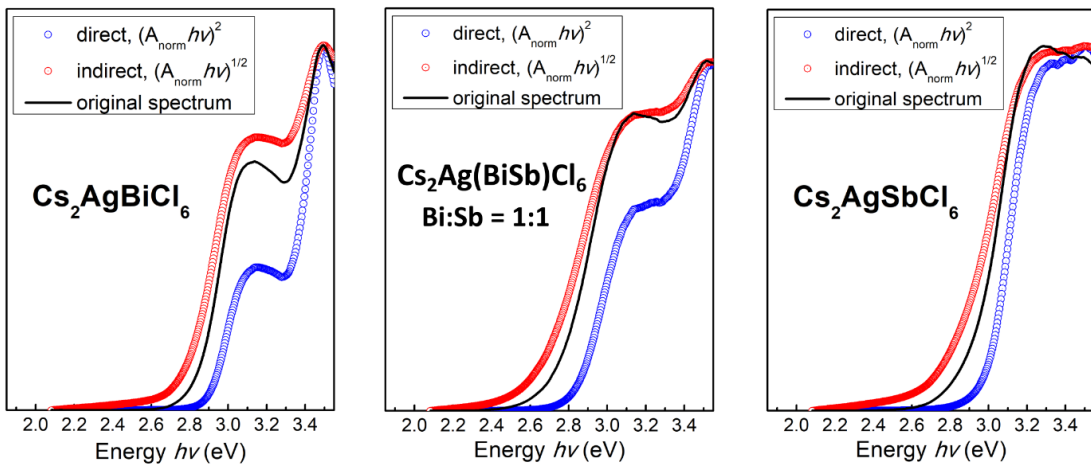


**Figure S5.** Normalized absorption spectra of  $\text{Cs}_2\text{AgBiCl}_6$ ,  $\text{Cs}_2\text{AgBi}_{0.5}\text{Sb}_{0.5}\text{Cl}_6$ , and  $\text{Cs}_2\text{AgSbCl}_6$  double perovskites presented in original form (solid black lines) and in Tauc coordinates for direct transitions (blue open rings) and indirect transitions (red open rings).

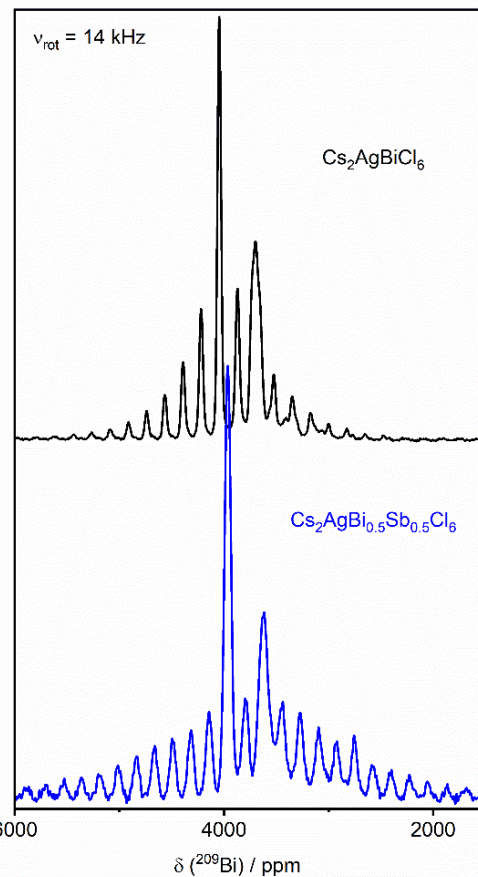


**Figure S6.**  $^{209}\text{Bi}$  MAS NMR spectra of  $\text{Cs}_2\text{AgBiCl}_6$  (upper black trace) and mixed  $\text{Cs}_2\text{AgBi}_{0.5}\text{Sb}_{0.5}\text{Cl}_6$  (lower blue trace) double perovskites. The presence of an unidentified secondary Bi phase is observed between 3600-3800 ppm, unfortunately overlapping with the residual first-order spinning sideband of the dominant double perovskite.

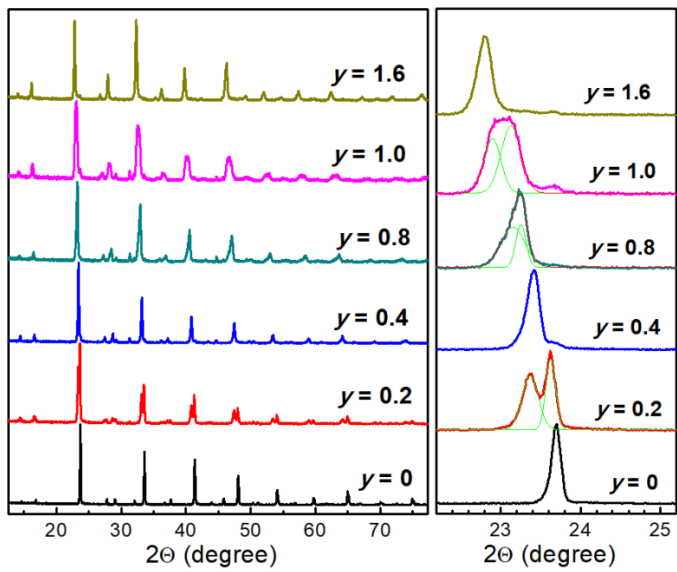


**Figure S7.** XRD patterns of the products of Cl-to-Br substitution in CABC double perovskites with a varied nominal ratio of  $y = \text{Br}/(\text{Cl}+\text{Br})$ .

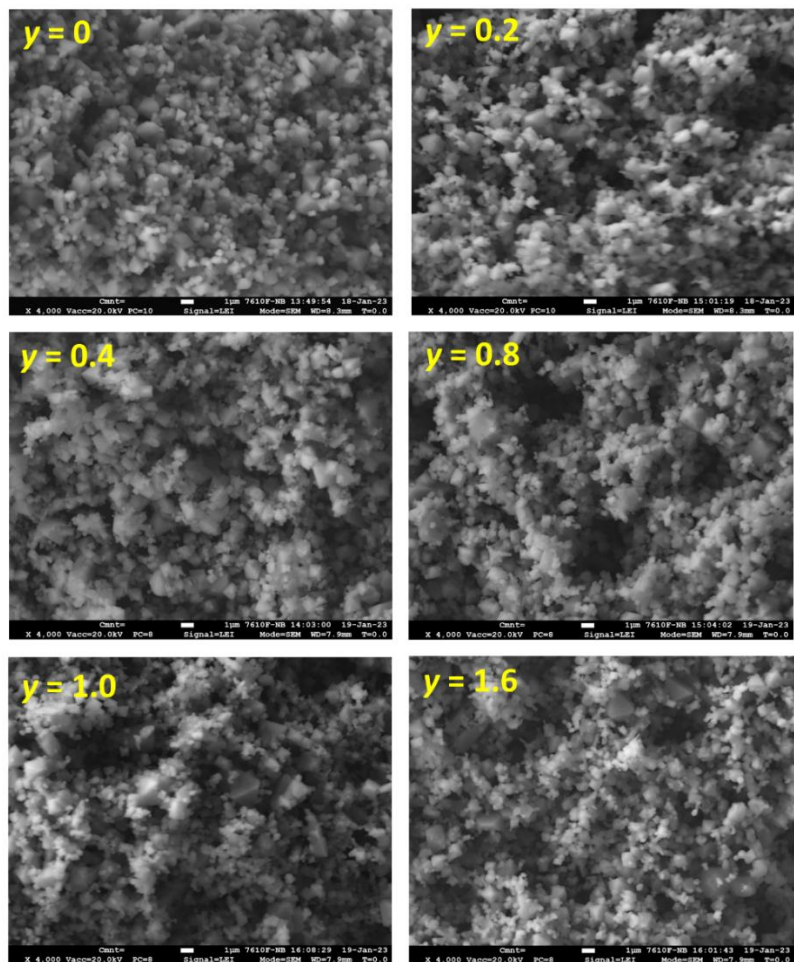


**Figure S8.** SEM images of the products of Cl-to-Br substitution in CABC double perovskites with a varied nominal ratio of  $y = \text{Br}/(\text{Cl}+\text{Br})$ .

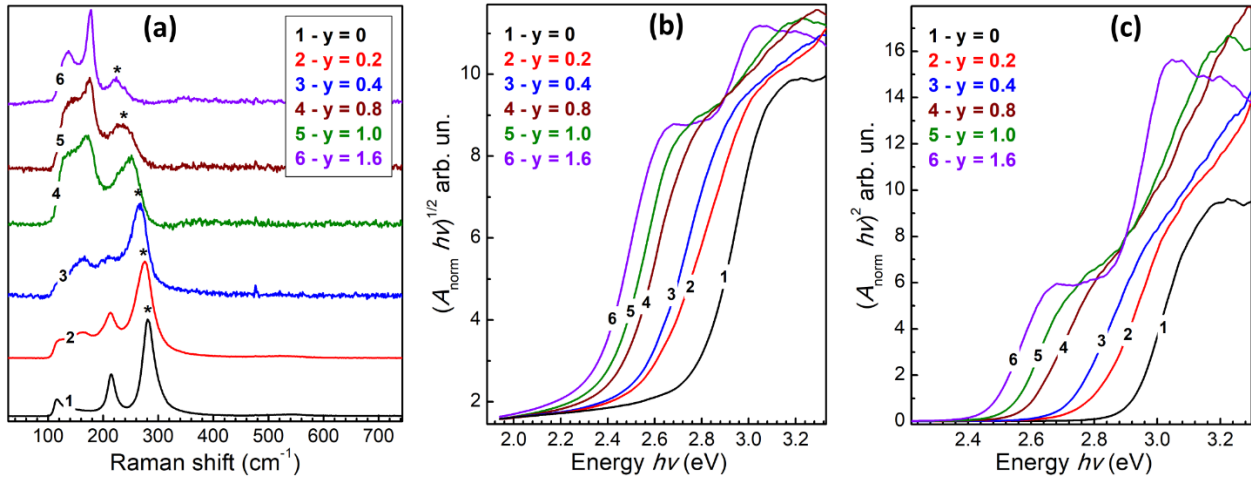


**Figure S9.** Raman spectra (a) and absorption spectra (b,c) of the products of Cl-to-Br substitution in CABC double perovskites with a varied nominal ratio of  $y = \text{Br}/(\text{Cl}+\text{Br})$ . In (a) the position of the highest-energy peak  $\nu$  is marked by an asterisk. Absorption spectra are presented in Tauc coordinates for indirect transitions (b) and direct transitions (c).

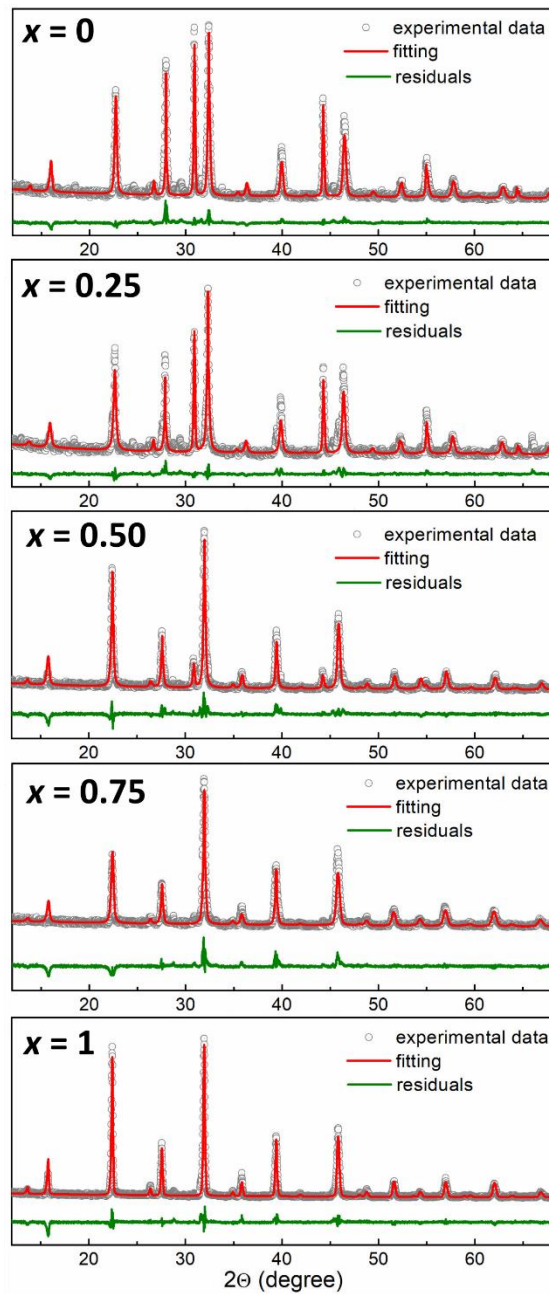


**Figure S10.** XRD profiles for the products of interaction between NaBr and  $\text{Cs}_2\text{AgBi}_x\text{Sb}_{1-x}\text{Cl}_6$  (CABSC) double perovskites with varied nominal Bi fraction  $x$ : gray scatter shows experimental data, solid red lines represent Rietveld refinement of the XRD patterns, green line shows the difference between experimental data and fitting curves (residuals).

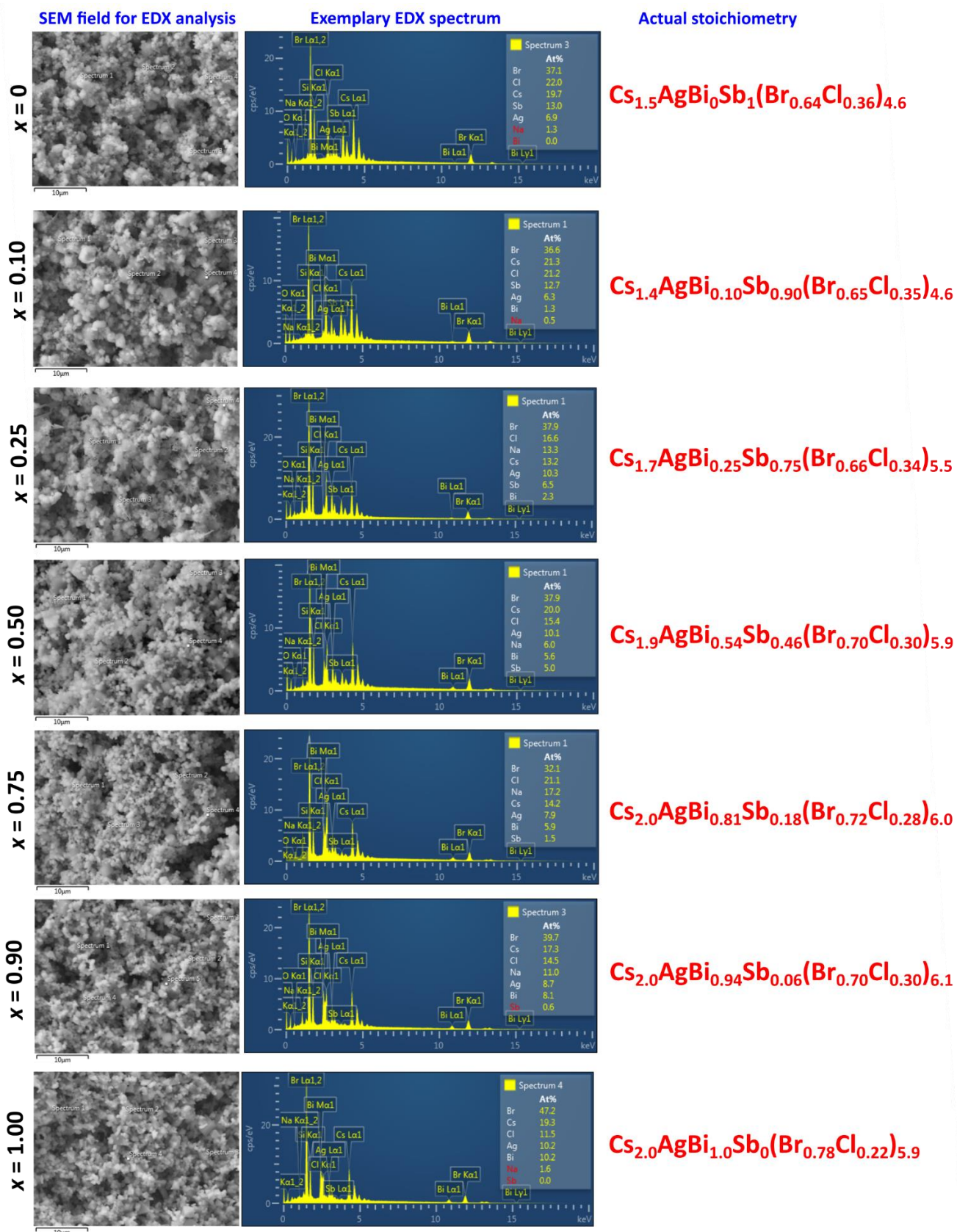


**Figure S11.** SEM of sample areas used for the EDX analysis, exemplary EDX spectra, and actual stoichiometries derived from EDX data for the products of Cl-to-Br substitution in CABSC perovskites.

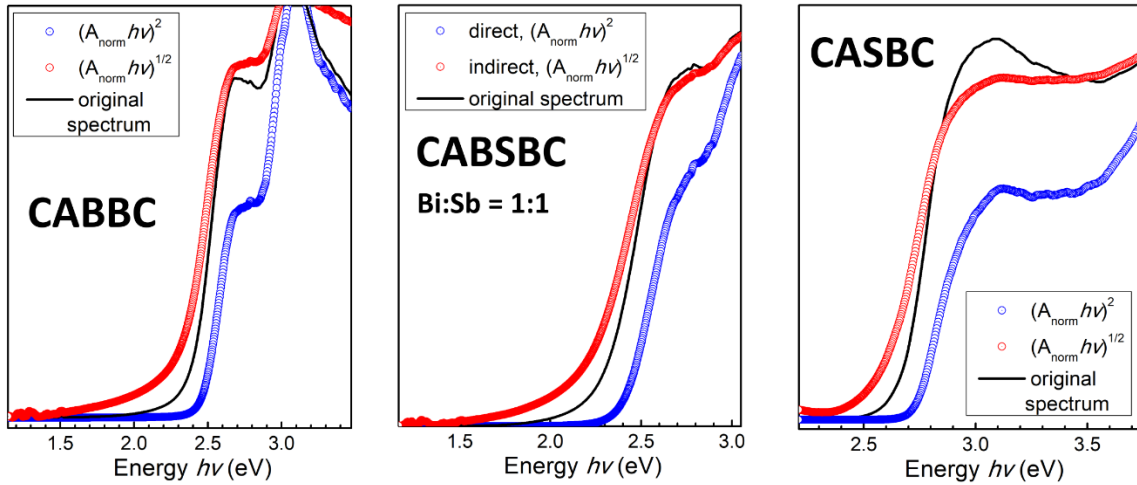


**Figure S12.** Normalized absorption spectra of CABBC, CABSBC (Bi:Sb = 1:1), and CASBC presented in original form (solid black lines) and in Tauc coordinates for direct transitions (blue open rings) and indirect transitions (red open rings).

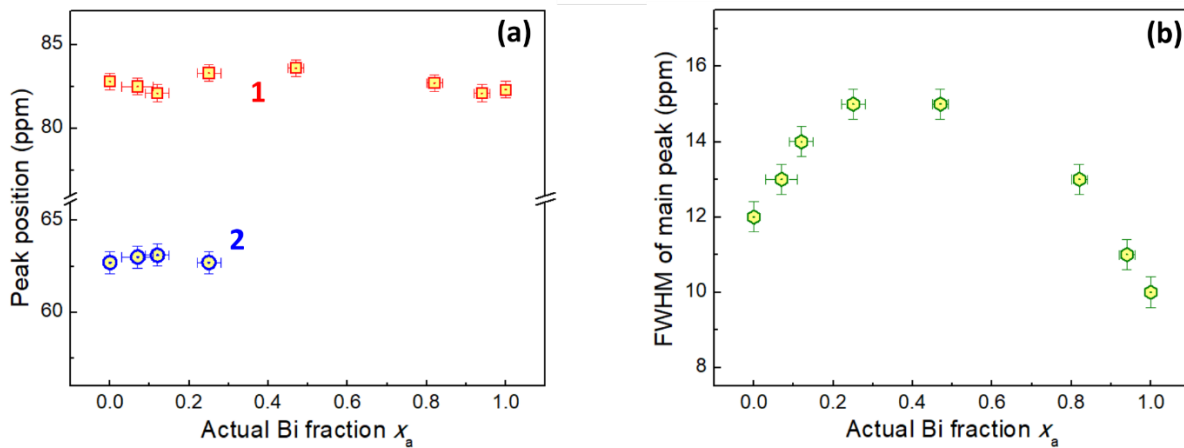


**Figure S13.** Positions of peaks (a) and FWHM of the main peak at 82-84 ppm (b) in  $^{133}\text{Cs}$  MAS NMR spectra of the products of anion exchange of CABSC perovskites with NaBr.

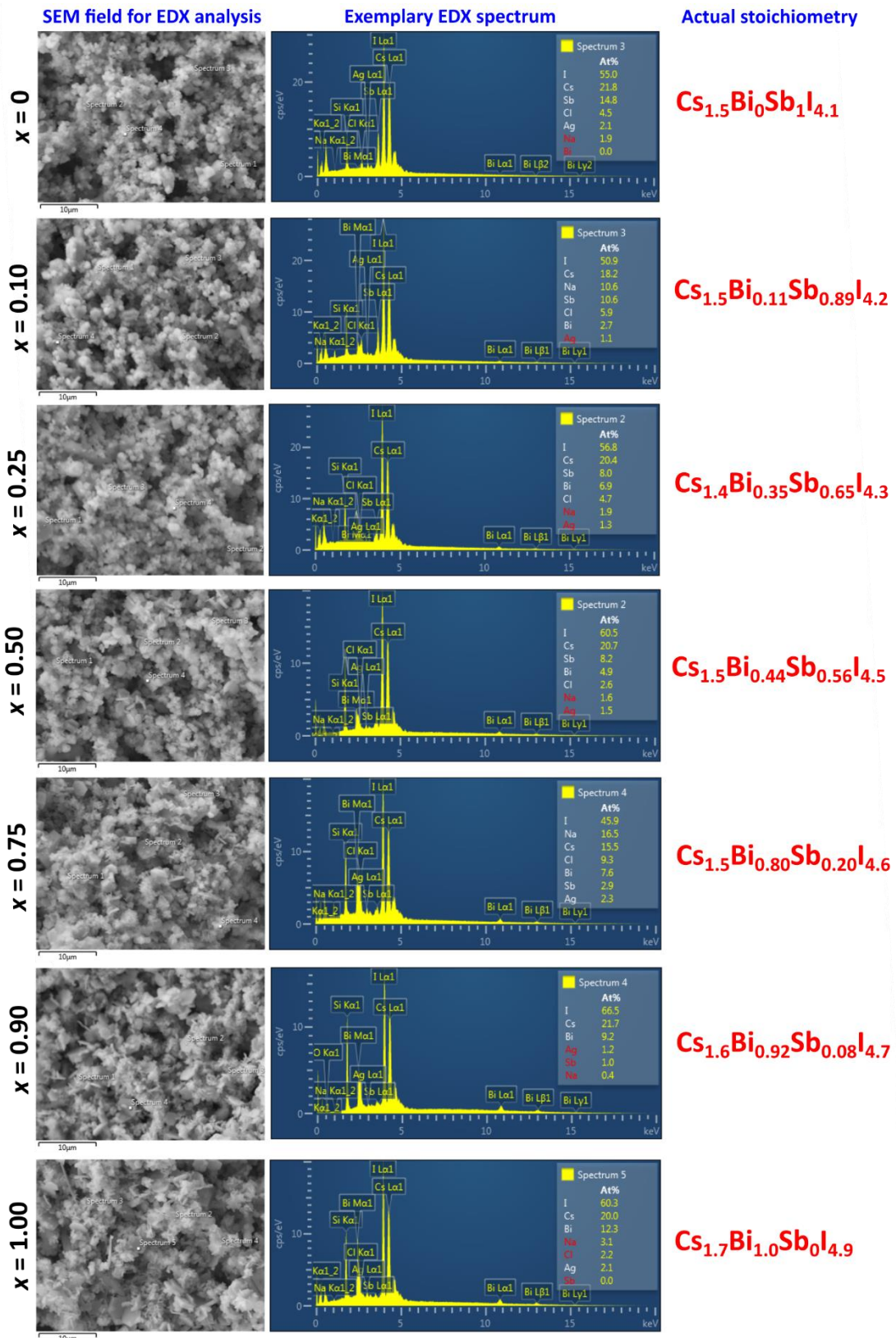


**Figure S14.** SEM of sample areas used for the EDX analysis, exemplary EDX spectra, and actual stoichiometries derived from EDX data for the products of Cl-to-I substitution in CABSC perovskites.

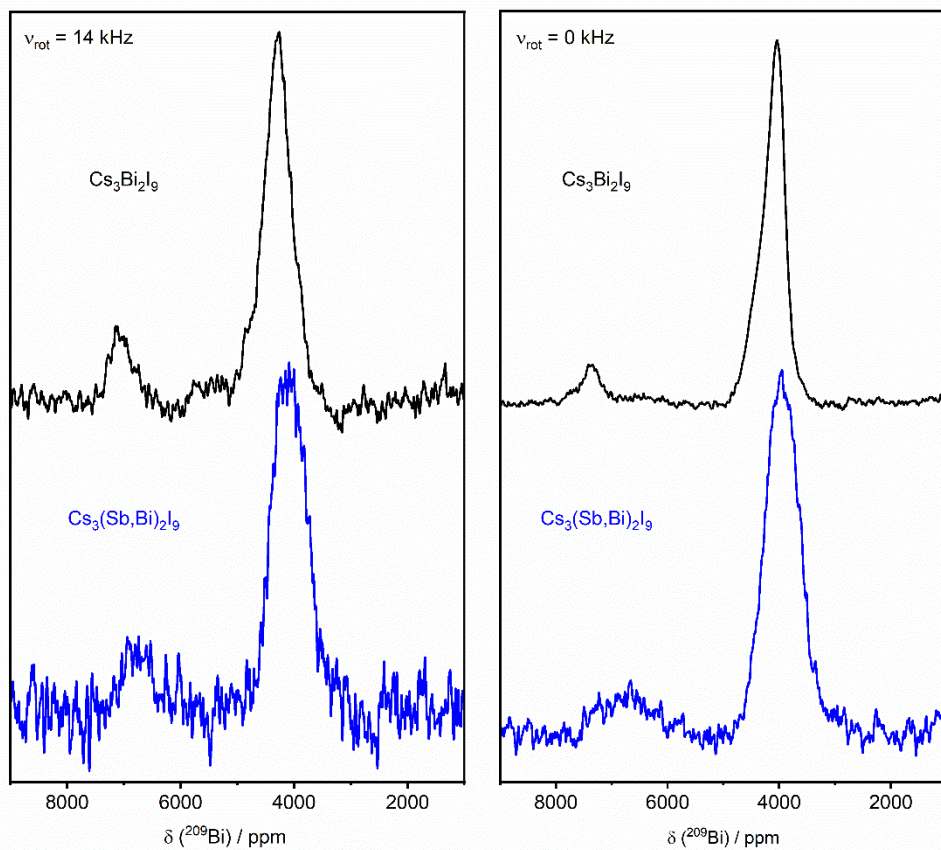


**Figure S15.**  $^{209}\text{Bi}$  MAS (left) and non-spinning (right) NMR spectra of  $\text{Cs}_3\text{Bi}_2\text{I}_9$  (upper black trace) and mixed  $\text{Cs}_3(\text{Sb},\text{Bi})_2\text{I}_9$  (lower blue trace) compounds.

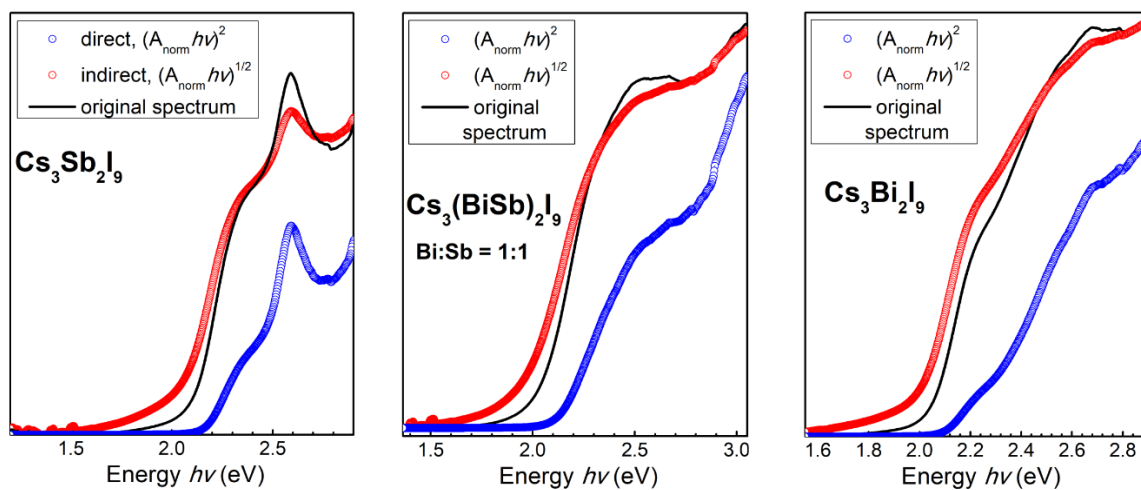


**Figure S16.** Normalized absorption spectra of CSI, CBSI (Bi:Sb = 1:1), and CBI presented in original form (solid black lines) and in Tauc coordinates for direct transitions (blue open rings) and indirect transitions (red open rings).